BIOCHEMISTRY
including biophysical chemistry & molecular biology
Article

Biochemistry **2010,** *49,* 7119–7130 7119
DOI: 10.1021/bi1004365

High-Affinity Interaction of Poly(ADP-ribose) and the Human DEK Oncoprotein Depends upon Chain Length†

Jörg Fahrer,[‡,§] Oliver Popp,[§] Maria Malanga,[⊥] Sascha Beneke,[§] David M. Markovitz,[@,#,+] Elisa Ferrando-May,[∥] Alexander Bürkle,[§] and Ferdinand Kappes*,[@]

[‡]*Institute of Pharmacology and Toxicology, University of Ulm Medical Center, Ulm, Germany,* [§]*Molecular Toxicology Group,* [∥]*Bioimaging Center, Department of Biology, University of Konstanz, Konstanz, Germany,* [⊥]*Department of Structural and Functional Biology, University Federico II of Naples, Naples, Italy,* [@]*Department of Internal Medicine, Division of Infectious Diseases,* [#]*Cellular and Molecular Biology Program, and* [+]*Program in Immunology, University of Michigan Medical Center, Ann Arbor, Michigan 48109*

Received March 23, 2010; Revised Manuscript Received July 2, 2010

ABSTRACT: Poly(ADP-ribose) polymerase-1 (PARP-1) is a molecular DNA damage sensor that catalyzes the synthesis of the complex biopolymer poly(ADP-ribose) (PAR) under consumption of NAD^+. PAR engages in fundamental cellular processes such as DNA metabolism and transcription and interacts noncovalently with specific binding proteins involved in DNA repair and regulation of chromatin structure. A factor implicated in DNA repair and chromatin organization is the DEK oncoprotein, an abundant and conserved constituent of metazoan chromatin, and the only member of its protein class. We have recently demonstrated that DEK, under stress conditions, is covalently modified with PAR by PARP-1, leading to a partial release of DEK into the cytoplasm. Additionally, we have also observed a noncovalent interaction between DEK and PAR, which we detail here. Using sequence alignment, we identify three functional PAR-binding sites in the DEK primary sequence and confirm their functionality in PAR binding studies. Furthermore, we show that the noncovalent binding to DEK is dependent on PAR chain length as revealed by an overlay blot technique and a PAR electrophoretic mobility shift assay. Intriguingly, DEK promotes the formation of a defined complex with a 54mer PAR ($K_D = 6 \times 10^{-8}$ M), whereas no specific interaction is detected with a short PAR chain (18mer). In stark contrast to covalent poly(ADP-ribosyl)ation of DEK, the noncovalent interaction does not affect the overall ability of DEK to bind to DNA. Instead the noncovalent interaction interferes with subsequent DNA-dependent multimerization activities of DEK, as seen in South-Western, electrophoretic mobility shift, topology, and aggregation assays. In particular, noncovalent attachment of PAR to DEK promotes the formation of DEK−DEK complexes by competing with DNA binding. This was seen by the reduced affinity of PAR-bound DEK for DNA templates in solution. Taken together, our findings deepen the molecular understanding of the DEK−PAR interplay and support the existence of a cellular "PAR code" represented by PAR chain length.

Poly(ADP-ribosyl)ation is a dramatic posttranslational modification of proteins conducted by the superfamily of poly(ADP-ribose) polymerases (PARPs) (*1*, *2*). PARP-1[1] is the best understood member of this class of enzymes and is responsible for ~90% of cellular poly(ADP-ribose) (PAR) formation after DNA damage (*3*). PARP-1 is crucial for the maintenance of genomic stability and plays an important role during DNA repair, in particular, base excision repair (BER) (*4*−*12*). Binding to DNA strand breaks activates PARP-1, which catalyzes the transfer of ADP-ribose moieties onto acceptor proteins under the consumption of NAD^+. The PAR which is thus formed is a highly complex biopolymer and was shown to interact in a noncovalent fashion with various proteins involved in DNA damage checkpoint control and repair and most likely also influences other biological processes (*6*). In turn, hydrolysis of PAR by the enzyme poly(ADP-ribose) glycohydrolase (PARG) also critically influences genomic stability and cellular survival (*13*, *14*). PAR binding is mediated by a consensus motif, which has been identified in crucial domains of many proteins and may therefore interfere with their respective functions (*15*). Lately, a zinc-finger motif was described by Ahel and co-workers that displays specific PAR binding activity and is present in some DNA repair-associated proteins (*16*). We recently showed that the well-known PAR-binding protein p53, a tumor suppressor protein that functions in double-strand break repair (*17*), exhibits a high binding affinity for PAR, with a K_D in the low nanomolar range (*18*). Noncovalent interaction between PAR and p53 has been demonstrated to inhibit both the sequence-specific and non-sequence-specific DNA binding of p53 in a PAR-dependent manner (*19*). Importantly,

†This work was supported by grants from the German Research Foundation (FOR 434 to A.B. and MA2385/2-3 to E.F.-M.). F.K. was supported by a William D. Robinson Fellowship from the Arthritis Foundation/Michigan Chapter and is a recipient of an Arthritis Foundation Postdoctoral Fellowship. Work in the laboratory of D.M.M. was supported by National Institutes of Health Grants R01-AI062248 and R01-AI087128 and by a Burroughs Wellcome Fund Clinical Scientist Award in Translational Research. The authors would like to thank the Konstanz Research School Chemical Biology (KoRS-CB) for financial and scientific support.

*To whom correspondence should be addressed: Department of Internal Medicine, Division of Infectious Diseases, University of Michigan Medical Center, 1150 W. Medical Center Dr., 5240 MSRB III, Ann Arbor, MI 48109. Telephone: (734) 936-8185. Fax: (734) 764-0101. E-mail: kappesferdinand1@gmail.com.

[1]Abbreviations: PAR, poly(ADP-ribose); PARP-1, poly(ADP-ribose) polymerase-1; BER, base excision repair; aa, amino acid; Topo I, topoisomerase I; EMSA, electrophoretic mobility shift assay; PARG, poly(ADP-ribose) glycohydrolase.

Published on Web 07/23/2010

several BER proteins harbor the PAR consensus motif, e.g., XRCC1, DNA ligase III, and DNA polymerase ε, underscoring the role of PAR in the spatiotemporal organization of BER (*15*, *20*, *21*). Very recently, interplay of the protein kinase ATM, an early DNA damage sensor, and PAR has been described, indicating that rapid and transient PAR formation may directly or indirectly activate the ATM signaling pathway (*22*).

Recently, we provided evidence that DEK, an abundant nonhistone chromosomal factor (*23*), is a PARP-1 substrate implicated in the repair of DNA strand breaks, assigning DEK a function in the PAR-dependent maintenance of genomic stability (*24*). Human DEK was initially discovered in a chimeric fusion protein with the nucleoporin CAN/NUP214 in a subset of patients with acute myeloid leukemia (AML) (*25*). Overexpression of *DEK* mRNA and DEK protein has subsequently been identified in a growing number of aggressive human tumors (*26*−*29*). Furthermore, high levels of DEK support cell immortalization and inhibit both senescence and apoptosis (*30*, *31*), and DEK overexpression itself was shown recently to be sufficient for HRAS-driven epithelial hyperplasia induction and epithelial transformation, classifying it as a bona fide oncogene (*32*, *33*). We further demonstrated that DEK is a true oncoprotein and a potential target for chemotherapy in malignant melanoma (*28*). Interestingly, DEK is also associated with several autoimmune disorders such as juvenile rheumatoid arthritis and systemic lupus erythematosus, thereby representing a major autoantigen (*34*).

The amino acid (aa) sequence of human DEK (375 aa) harbors a nuclear localization sequence (NLS) and four highly acidic stretches, shown to have inhibitor of histone acetyltransferase activity (INHAT) in vitro (*35*). DEK harbors two structurally and functionally distinct DNA-binding domains (*36*−*40*). The central domain, spanning aa 87−187, represents an unprecedented form of the DNA-binding motif SAP box, which consists of two SAP folds, with each of these folds being able to independently interact with dsDNA and to stimulate DNA-dependent protein−protein interactions (*36*, *41*, *42*). This domain mediates the characteristic DNA binding and folding feature of DEK, i.e., a predominantly structure-specific (four-way junction, supercoiled, distorted DNA) DNA binding activity, resulting in a general compaction of chromatin as well as DNA templates and the introduction of positive superhelical turns into closed circular DNA and chromatin templates in vitro (*36*, *38*, *39*, *42*, *43*). Interestingly, a SAP domain has also been identified via a PSI-BLAST search in plant PARP-1 (*44*). Similar to human DEK, PARP-1 is also capable of binding to unusual DNA structures such as cruciforms and loops (*45*, *46*). A second DNA-binding domain, located in the C-terminal region of DEK (aa 250−350), represents a winged-helix motif found in transcription factors of the E2F family and upon phosphorylation stimulates self-association of DEK molecules and/or other yet to be elucidated chromatin-associated factors (*36*, *37*, *47*).

DEK has been linked to a variety of intracellular activities, as it has been implicated in DNA replication (*43*) and RNA processing (*48*), as a positive (*28*, *49*, *50*) or negative (*31*, *51*−*54*) regulator of transcription, and as a participant in DNA double-strand repair (*24*). DEK is a target of a plethora of post-translational modifications, and these most likely regulate or integrate its various intra- and extracellular activities. In fact, phosphorylation (*24*, *37*, *55*), acetylation (*56*), and poly(ADP-ribosyl)ation (*24*, *52*) were shown to affect DEK's subcellular and subnuclear distribution and interaction partners.

Strikingly, DEK shares several functional similarities with HMGB1 (high-mobility group B protein 1) (*40*), which is a known acceptor for covalent poly(ADP-ribosyl)ation (*57*). Moreover, both PARP-1 and DEK have been detected in a HeLa cell chromatin fraction enriched for the variant histone macroH2A and were found to coreside on chromatin fragments released by micrococcal nuclease, underscoring their close connection (*24*, *58*). Furthermore, we showed that DEK not only is a target for covalent poly(ADP-ribosyl)ation but also binds PAR in a noncovalent fashion (*24*). We have demonstrated that the binding affinity of PAR for specific proteins is very high and that this interaction is very selective with respect to PAR chain length and the binding partner (*18*). Here, we identify specific PAR binding motifs within the DEK primary sequence and quantify this noncovalent interaction as a function of chain length. Moreover, we address the question of whether the noncovalent binding of PAR to DEK affects the well-described functional properties of DEK.

MATERIALS AND METHODS

Materials. Human PARP-1 was expressed in Sf9 insect cells and purified as described previously (*18*). His-tagged full-length DEK and DEK fragments were also produced in insect cells and purified as previously described (*36*, *37*). It is important to note that recombinant DEK purified from the baculovirus system is highly phosphorylated. Throughout this work, recombinant His-DEK was used either in its phosphorylated form (Figures 1−3) or in its dephosphorylated form (after treatment with λ-phosphatase), for DNA binding studies (Figures 4−6). Phosphorylation moderately reduced the overall PAR binding capacity of DEK but did not interfere with the observed preferential binding selectivity of DEK for the long chain PAR polymer (see Figure 4A and Figure S2 of the Supporting Information). The DEK fragment of residues 68−226 was expressed and purified from *Escherichia coli* as previously described (*42*) and is therefore unphosphorylated (*24*, *37*, *59*). DEK peptides 195−222, 158−181, and 99−119 were custom-synthesized by Coring System Diagnostix GmbH, and peptides 329−352 and 314−334 were synthesized using an Fmoc/tBu-based solid phase method. Affinity-purified polyclonal DEK antibodies were used as reported previously (*24*, *37*). Mouse monoclonal antibody 10H, which recognized PAR, was purified from the culture supernatant of 10H hybridoma cells (*59*).

In Vitro PAR Synthesis and Purification. PAR was synthesized essentially as described previously (*18*). Briefly, 150 nM human PARP-1 was incubated with 1 mM NAD^+, 1 mM DTT, 60 μg/mL histone H1, 60 μg/mL histone type IIa, and 50 μg/mL octameric "activator" oligonucleotide GGAATTCC in a total volume of 20 mL containing 1× reaction buffer [100 mM Tris-HCl (pH 7.8) and 10 mM $MgCl_2$]. After 15 min, the PAR produced was precipitated by addition of 20 mL of 20% TCA, and the pellet was washed several times with ice-cold 99.8% ethanol. PAR was further purified according to the method of Malanga et al. (*60*) and finally precipitated with ethanol overnight.

Terminal Biotinylation and Neutravidin ELISA. PAR was dissolved in sodium acetate buffer (pH 5.5) containing 4 mM biocytin hydrazide and biotinylated under reductive amination conditions for 8 h as described previously (*18*). Following dialysis and ethanol precipitation, the PAR concentration was determined using UV absorbance at 258 nm (*61*). Successful terminal labeling of PAR chains was checked using a neutravidin ELISA.

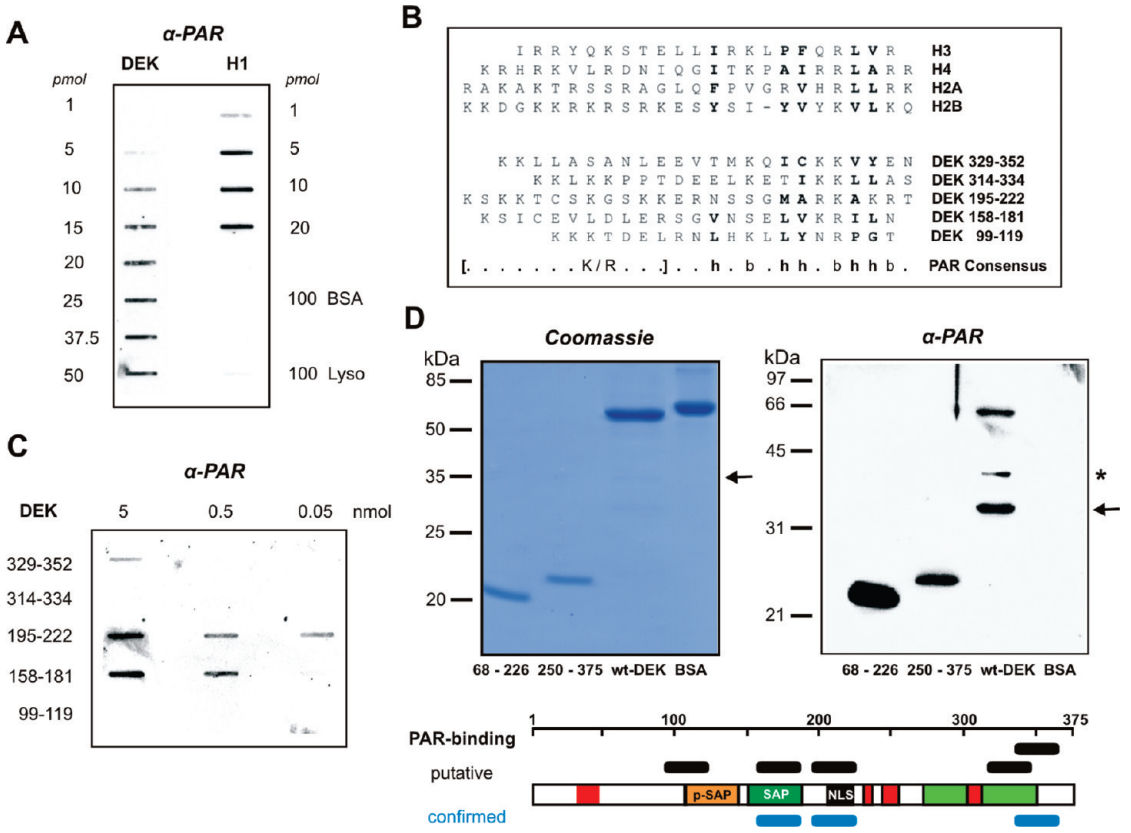

FIGURE 1: Mapping of PAR−interaction modules in the DEK protein. (A) DEK specifically interacts with PAR. Increasing amounts of recombinant DEK and histone H1 (positive control), as well as BSA, and lysozyme in excess (negative controls) were slot-blotted onto a nitrocellulose membrane. Following incubation with PAR (1 μM), the membrane was treated with high-salt washes to disrupt nonspecific binding. Bound polymer was immunodetected using specific PAR antibodies (10H). (B) Alignment of the PAR binding consensus sequence with the DEK amino acid sequence. The top panel shows PAR-binding motifs identified in different histones according to Pleschke et al. (*15*). The bottom panel shows putative PAR-binding motifs in DEK found by alignment according to the consensus sequence: h, hydrophobic; b, basic amino acids. (C) PAR binding to DEK peptides. Decreasing amounts of DEK peptides synthesized according to the alignment were slot-blotted onto a nitrocellulose membrane. After incubation with biotinylated PAR (50 nM), the membrane was treated with high-salt washes to disrupt nonspecific binding. Bound polymer was visualized using streptavidin-POD. (D) PAR binding analysis using His-tagged DEK fragments. The respective fragments (aa 68−226, aa 250−375, and aa 1−375) and BSA (BSA) as a negative control were subjected to 15% SDS−PAGE and visualized by Coomassie staining (100 pmol, left panel) or analyzed using a PAR overlay blot (15 pmol, right panel). After semidry blotting and incubation with free biotinylated PAR (0.4 μM), the bound polymer was visualized as described for panel A. The described 35 kDa breakdown product of wt-DEK is denoted with an arrow. An additional intermediate breakdown product, capable of PAR binding, is denoted with an asterisk. The scheme summarizes the putative (black) and experimentally confirmed (blue) PAR-binding domains in the DEK amino acid sequence (red boxes, acidic domains; orange, pseudo-SAP box; green, SAP box; black, nuclear localization sequence; light green, second DNA binding/multimerization domain).

Biotin-labeled PAR samples diluted in 50 mM $NaHCO_3$ (pH 7.5) were transferred to ELISA plates and incubated for 1 h at room temperature. Captured biotinylated PAR was detected with primary antibody 10H (4 μg/mL) in conjunction with a secondary peroxidase-conjugated anti-mouse IgG (DakoCytomation, 1:2000) and visualized in a Tecan GeniosPlus ELISA reader. A biotinylated PAR standard was synthesized in the presence of NAD^+ and 6-biotin-17-NAD^+ (15:1 ratio), resulting in the incorporation of biotinylated ADP-ribose units into the polymer (*62*). An excess of unlabeled PAR served as a specificity control to rule out nonspecific PAR binding. In addition, terminal biotin labeling of PAR chains was assessed after electrophoretic separation and semidry blotting by incubation with streptavidin-POD (1:2000).

HPLC Fractionation of Biotinylated PAR. Separation of biotinylated PAR was conducted on a Shimadzu LC-8A HPLC system equipped with a semipreparative DNA Pac PA100 column (DIONEX). PAR was eluted according to chain length using a multistep NaCl gradient in 25 mM Tris-HCl (pH 9.0) and collected manually after UV detection at 258 nm (*18*, *63*). Biotin-labeled ADP-ribose polymers were characterized on modified sequencing gels (*64*) and visualized using GELCODE Color silver stain (Pierce) as described previously (*60*).

PAR Overlay Blot. Increasing amounts of recombinant DEK (1−50 pmol), histone H1 (1−20 pmol), and BSA and lysozyme (100 pmol each) were vacuum-aspirated onto a nitrocellulose membrane (Amersham Biosciences) using a slot-blot manifold (Schleicher & Schuell). To map the binding of PAR to specific DEK domains, His-tagged DEK fragments (15 pmol for the PAR overlay blot; 100 pmol for Coomassie staining) were separated by 15% SDS−PAGE and stained by Coomassie or transferred onto a nitrocellulose membrane by semidry blotting. Membranes were incubated with Tris-buffered saline and Tween 20 (TBS-T) containing 1 nmol (0.4 μM) of purified PAR for 1 h. Membranes were subsequently washed in TBS-T and 1 M NaCl and blocked with 5% (w/v) skim milk powder in TBS-T. Detection of bound PAR was performed using 10H antibodies and secondary antibodies (goat α-mouse/HRP). Bands were visualized in the FujiLAS1000 device using enhanced chemiluminescence, and blots were evaluated with AIDA (Raytest).

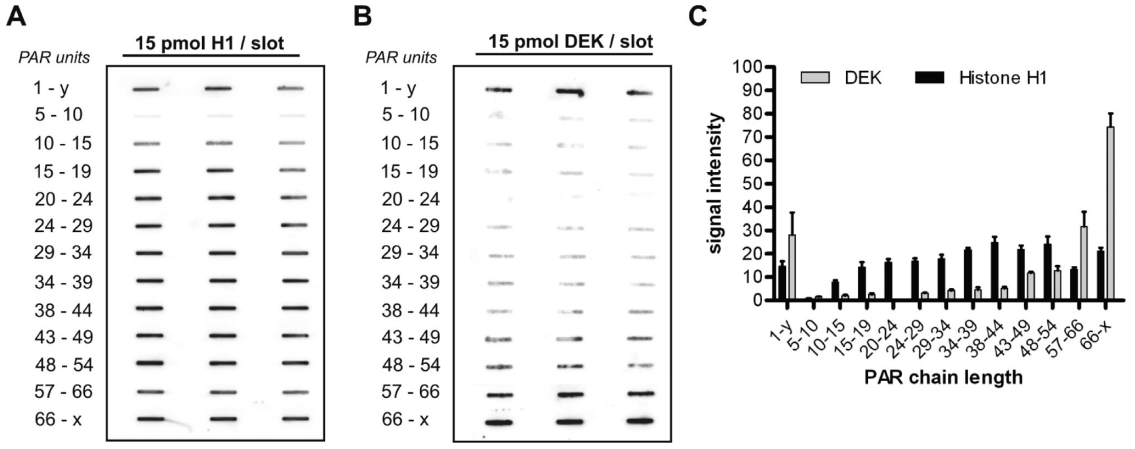

FIGURE 2: Interaction of fractionated PAR and immobilized DEK. DEK preferentially binds long chains of PAR. For each binding assay, 15 pmol of full-length DEK or histone H1 was vacuum aspirated on a nitrocellulose membrane and cut into strips, followed by incubation with 500 pmol of the respective PAR fraction (0.25 μM; $1-y$ denotes unfractionated PAR). Each reaction was run in triplicate. Nonspecific binding was abrogated by high-salt washes, and bound PAR chains were detected using PAR-specific antibodies (10H). (A) Binding of fractionated PAR to immobilized histone H1. (B) Binding of fractionated PAR to immobilized DEK. (C) Densitometric evaluation of slot blots. The signal intensity is indicated in arbitrary units. The bars represent means ± the standard error of the mean of triplicate determinations.

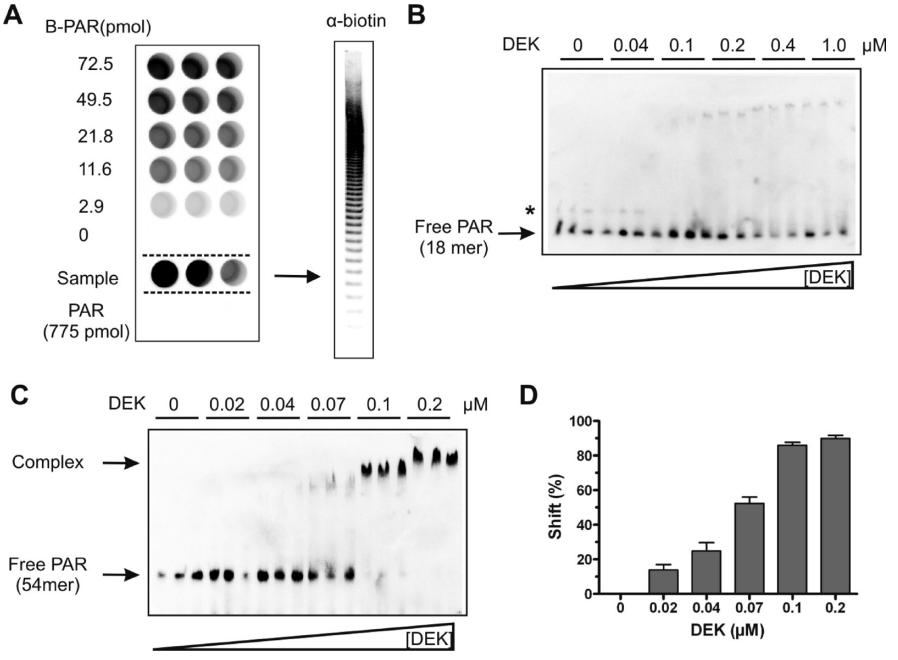

FIGURE 3: Specific end labeling of PAR chains and PAR EMSA. (A) Characterization of terminal biotin labeling by a neutravidin ELISA. Biotinylated PAR was captured in the neutravidin-coated wells (left panel) and detected using PAR-specific antibodies (10H). B-PAR denotes the biotinylated PAR standard, with an end-labeled PAR sample using biocytin hydrazide (171, 86, and 17 pmol from left to right). The end-labeled PAR sample was also analyzed by a native 20% PAGE followed by semidry transfer on a nylon membrane. Biotinylated PAR chains were visualized by streptavidin-POD. (B and C) Interaction of size-fractionated PAR and DEK in solution. Biotin-labeled PAR of a defined chain length was incubated with increasing concentrations of DEK and subjected to native PAGE followed by semidry blotting. Bound polymer and free polymer were detected using streptavidin-POD. Free and complexed PAR is denoted with an arrow. In panel B, a minor cross contamination with PAR of a longer chain length is denoted with an asterisk. (B) Binding of DEK to a short PAR 18mer (250 fmol/lane). (C) Binding of DEK to long PAR chains (54mer, 125 fmol/lane). (D) Quantitative evaluation of DEK gel shifts. The shift (%) was calculated as follows: (signal intensity of complexed PAR)/(signal intensity of complexed PAR + signal intensity of free PAR). Data are expressed as means ± the standard error of the mean of triplicate determinations from two independent experiments.

Equimolar amounts of synthetic DEK peptides were dissolved in PBS and slot-blotted with the indicated concentrations onto a nitrocellulose membrane. After incubation with biotinylated PAR (50 nM in TBS-T), the membrane was washed three times with 1 M NaCl in TBS-T and blocked for 1 h in 5% skim milk powder in TBS-T. Subsequently, PAR binding was detected after incubation with streptavidin-POD (1:5000) in TBS-T for 1 h employing enhanced chemiluminescence.

To assess the binding of separated PAR chains to immobilized DEK, 15 pmol of recombinant protein was transferred onto nitrocellulose membranes using a slot-blot apparatus. The membranes were cut into strips and incubated with 500 pmol (0.25 μM) of the respective ADP-ribose fraction in TBS-T at 4 °C overnight. After high-stringency wash steps in TBS-T and 1 M NaCl, strips were blocked and bound polymer was detected using 10H antibodies as described above.

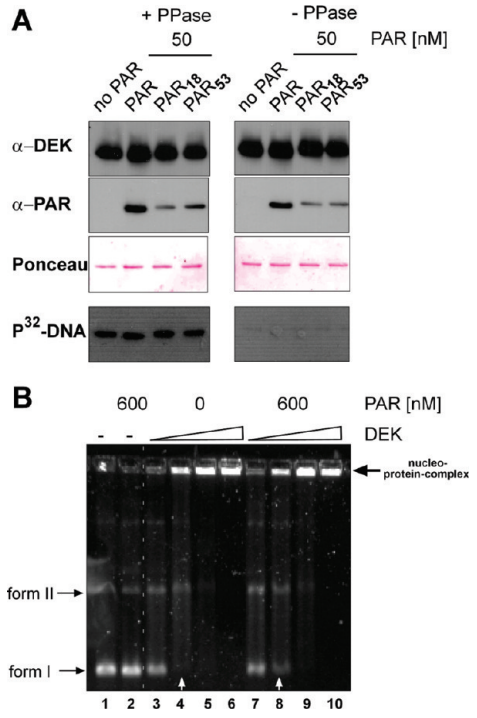

FIGURE 4: Noncovalent binding of PAR does not affect the overall DNA binding of DEK. (A) PAR overlay. Four hundred nanograms of dephosphorylated (+PPase, left panel) or phosphorylated (−PPase, right panel) His-DEK per lane was blotted to a nitrocellulose membrane, and the membrane was cut into strips and incubated with 50 nM unfractiontated PAR, short chain PAR (18mer), or long chain PAR (53mer) overnight (see also Figure S2 of the Supporting Information). Strips were subsequently probed with DEK (α-DEK) or PAR-specific antibodies (α-PAR, 10H). As a loading control, Ponceau S staining is shown. The bottom panel shows South-Western analysis. After being blocked and renatured, the individual strips were incubated with radioactively labeled SV40 DNA prior to detection of binding by autoradiography. (B) EMSA. Thirty nanograms of SV40 DNA was incubated with increasing amounts (100, 200, 400, or 800 ng) of either untreated or PAR-treated DEK, analyzed on a 0.6% agarose gel, and visualized by SYBRGold staining: form I, supercoiled DNA; form II, relaxed DNA. The arrow indicates DEK-specific large nucleoprotein complexes, which remain in the wells of the gel because of their high molecular weight. White arrows point to quantitative differences in the presence of form I DNA in samples with or without prior PAR treatment.

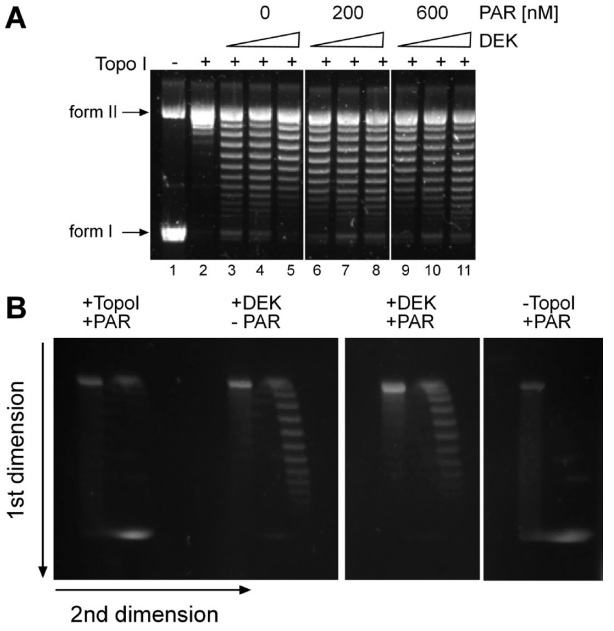

FIGURE 5: DEK's supercoiling activity is moderately influenced by noncovalent PAR interaction. (A) DNA topology assay. Seventy nanograms of SV40 DNA was incubated with 200, 400, or 800 ng of His-DEK in the presence of 200 or 600 nM PAR and topoisomerase I. The samples were then deproteinized by Proteinase K treatment, and the DNA was purified and analyzed by 0.8% agarose gel electrophoresis followed by SYBRGold staining: form I, supercoiled DNA; form II, relaxed DNA. (B) Two-dimensional topology assay. The DNA topology reaction was performed as described for panel A, and the deproteinized and purified DNA was separated by standard agarose gel electrophoresis in the first dimension (from top to bottom). Subsequently, the gel was incubated with 0.25 mg/mL chloroquine for 2 h and rotated by 90°, and after a run in the second dimension (from left to right), DNA was visualized by SYBRGold staining.

PAR Sequence Alignment. Putative PAR-binding sequences in DEK were aligned with the consensus PAR binding motif as reported previously (*15*).

Avidin Affinity Purification of Biotinylated PAR. End-biotinylated separated PAR chains were affinity-purified using SoftLink Soft Release Avidin Resin (Promega) before being used in EMSA studies. Briefly, biotinylated polymer was diluted to 2 mL in bind and wash (BW) buffer comprising 50 mM Tris-HCl (pH 8.0) and 50 mM NaCl and loaded onto the avidin column. After collection of the flow-through, the column was rinsed with 6 mL of BW buffer, and bound biotinylated PAR chains were gently eluted in 1 mL steps using a solution of 5 mM D-(+)-biotin. The purification process was analyzed by native 20% PAGE, and end-labeled PAR was detected using streptavidin-POD and enhanced chemiluminescence. The concentration of affinity-purified PAR was assessed by native PAGE using a biotinylated 49mer DNA oligonucleotide (Invitrogen) as the standard.

PAR EMSA. To characterize PAR−protein complexes in solution, we developed a PAR EMSA (*18*). Varying amounts of recombinant His-DEK were incubated in an appropriate volume of 10 mM Tris-HCl (pH 7.4) and 1 mM EDTA for 10 min at 25 °C before affinity-purified PAR of a defined chain length (18mer and 54mer, respectively) was added. Complex formation was allowed to proceed for 20 min at 25 °C until equilibrium was reached. Subsequently, the reaction mixture was supplemented with 10× loading dye resulting in a final volume of 25 μL. The samples were subjected to native 5% PAGE for 2.5 h at 160 V to separate free and bound ADP-ribose polymer. Thereafter, samples were blotted onto a nylon membrane by semidry transfer at 20 V for 50 min followed by heat fixation at 90 °C for 1 h. After being blocked with 2% BSA in TBS-T for 1 h, biotinylated ADP-ribose chains were detected by incubation with streptavidin-POD (1:2000 in blocking solution) for 1 h. Blots were visualized using a FujiLAS 1000 imager, and quantification was performed using AIDA. The shift (%) was determined as follows: (signal intensity of complexed PAR)/(signal intensity of complexed PAR + signal intensity of free PAR). The data obtained were analyzed using GraphPad Prism 4, and K_D values were calculated by using a sigmoidal dose−response curve with a variable slope. Curves were fitted using nonlinear regression (see Figure S5 of the Supporting Information).

EMSA, Topology, Aggregation Assay, and South-Western Analyses of Recombinant His-DEK. EMSA and topology assays were conducted as described previously (*24*, *36*). Recombinant His-DEK, purified from insect cells, was dephosphorylated with λ-phosphatase (New England Biolabs) prior to utilization. His-DEK was incubated with either unfractionated PAR or PAR of the indicated chain length and concentrations as specified

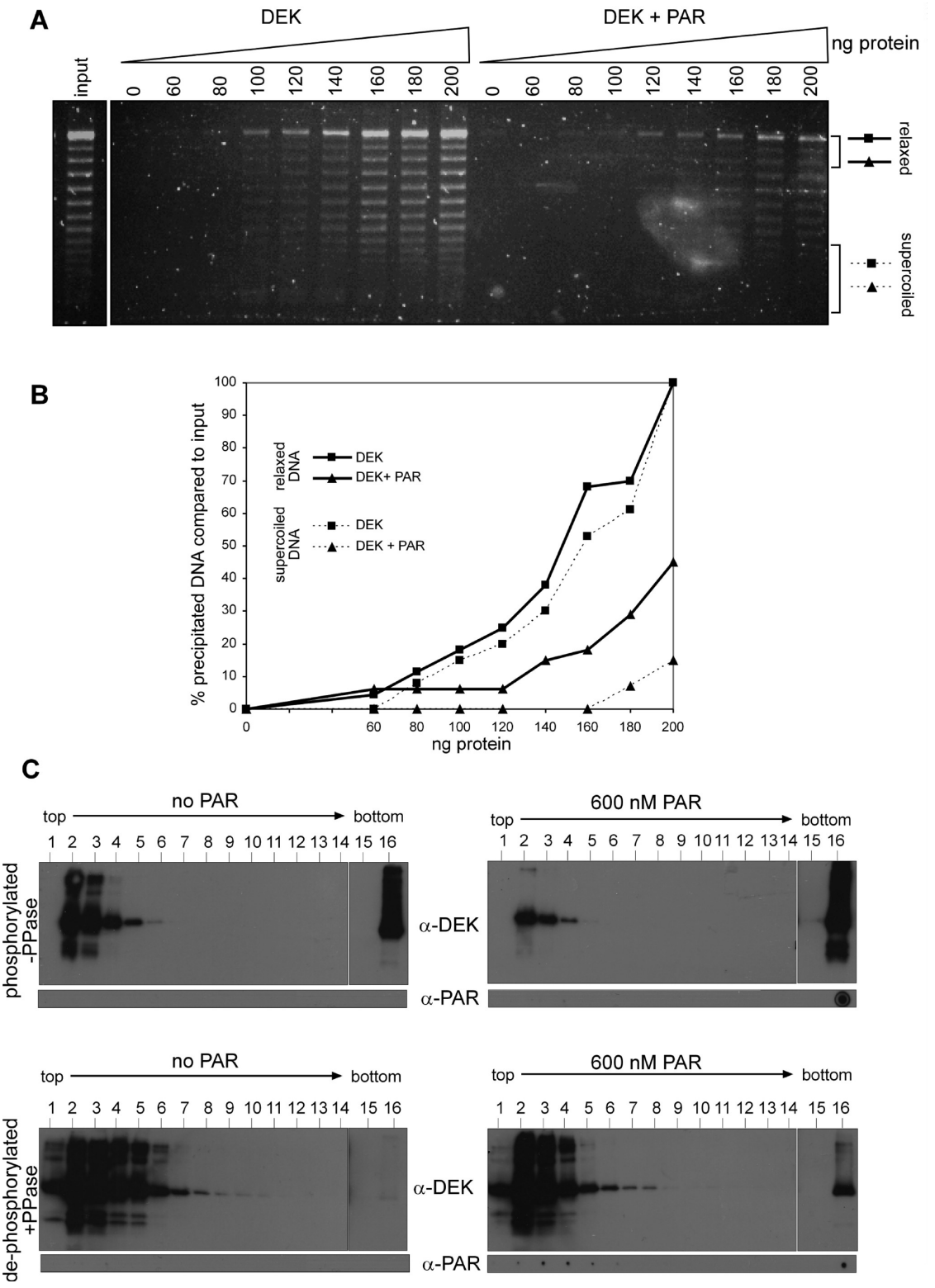

FIGURE 6: PAR attenuates DEK's affinity for highly supercoiled DNA templates by competitively stimulating the self-association activity of DEK molecules. (A) In the DEK aggregation assay, 0, 60, 80, 100, 120, 140, 160, 180, or 200 ng of His-DEK was incubated with 20 ng of partially relaxed SV40 DNA in the presence or absence of 600 nM PAR in a total volume of 30 μL. After incubation for 20 min at room temperature, samples were centrifuged for 15 min and pellets (i.e., precipitated material) were analyzed by 0.8% agarose gel electrophoresis and SYBRGold staining. (B) DEK-dependent precipitation of relaxed DNA topoisomeres (indicated by solid lines) or strongly superhelical topoisomers (dashed lines) was further analyzed by densitometry and is expressed as a percentage of precipitated DNA compared to input. (C) Sucrose density gradient analysis. Phosphorylated (−PPase) or dephosphorylated (+PPase) His-DEK was incubated in the presence (right panels) or absence (left panels) of 600 nM unfractionated PAR and subjected to sedimentation analysis on 5 to 40% sucrose density gradients. Individual fractions of the gradients were analyzed by SDS−PAGE and immunoblotting for DEK (α-DEK) or the dot-blot method using PAR-specific antibodies (α-PAR).

for the individual experiment for 20 min at room temperature prior to the start of the reaction. Individual samples were further supplemented with indicated PAR concentrations throughout the reactions. South-Western analyses were performed to investigate

Table 1: Comparison of K_D Values Obtained via an EMSA

protein	16/18mer PAR K_D (M)	55/54mer PAR K_D (M)
XPA	no binding	$3.2 \times 10^{-7} \pm 7.7 \times 10^{-9}$
p53	$2.5 \times 10^{-7} \pm 3.8 \times 10^{-8}$	$1.3 \times 10^{-7} \pm 4.2 \times 10^{-9}$
DEK	no binding	$6.1 \times 10^{-8} \pm 5.2 \times 10^{-9}$

DNA binding of DEK upon noncovalent PAR incubation and were conducted as described recently (*37*). Briefly, indicated amounts of His-DEK were separated via 10% SDS−PAGE and blotted onto a nitrocellulose membrane. Individual lanes were cut into strips and incubated overnight in TBS-T with PAR at the indicated concentrations in a total volume of 2 mL. Following three wash steps with TBS-T containing 1 M NaCl, the strips were blocked with 5% skim milk powder in 50 mM Tris-HCl (pH 7.5), 50 mM NaCl, 1 mM DTT, and 1 mM EDTA for 1 h at room temperature. As a probe, HinfI-digested, end-labeled SV40 DNA was used. After incubation for 1 h, the individual strips were washed collectively five times with 10 mM Tris-HCl (pH 7.5), 50 mM NaCl, 1 mM DTT, and 1 mM EDTA and subjected to autoradiography followed by immunoblotting. Aggregation assays, a measure of DNA-dependent multimerization of SAP box proteins, were performed as reported previously (*24*), using PAR incubation procedures described above. Two-dimensional DNA topology assays were conducted to identify the orientation of supercoils introduced and were essentially performed as described previously (*42*).

Sucrose Density Gradient Analysis. Sedimentation analysis of DEK was conducted as described previously (*36*, *37*). Briefly, 1500 ng (31 pmol) of recombinant His-DEK was either treated with λ-phosphatase (+PPase) or left untreated (−PPase). Both DEK preparations were subsequently incubated with 600 nM unfractionated PAR (in a total volume of 100 μL), or without PAR, for 30 min at room temperature and layered on top of a 5 to 40% sucrose density gradient [150 mM NaCl, 20 mM Tris-HCl (pH 7.5), 1 mM EDTA, 1 mM $MgCl_2$, and 10 mM sodium bisulfite]. After centrifugation for 12 h at 36000 rpm (SW-41), the gradient was fractionated from the top in fractions containing 700 μL; 100 μL of each fraction was spotted onto a nitrocellulose membrane using a dot-blot apparatus and further subjected to immunoblotting using PAR-specific antibodies (10H). The remaining 600 μL was processed for SDS−PAGE and further analyzed by immunoblotting using DEK-specific antibodies.

RESULTS

Mapping of DEK Domains Involved in Noncovalent PAR Interaction. We have recently shown that DEK is covalently modified with PAR during apoptosis or genotoxic stress, and our initial data suggested that DEK is also capable of interacting in a noncovalent fashion with free PAR polymers (*24*). To detail the specificity of the latter interaction, we used a slot-blot approach. Increasing amounts of recombinant DEK and histone H1, a well-known PAR-binding protein, were transferred onto a nitrocellulose membrane followed by PAR incubation and high-salt washes. Immobilized DEK interacted with PAR in a concentration-dependent manner (Figure 1A). Histone H1, as expected, exhibited even stronger binding, whereas the negative controls BSA and lysozyme, which were supplied in excess, did not bind. To identify potential PAR interaction sites, the DEK peptide sequence was aligned with the PAR consensus binding motif (*15*). Five putative PAR binding sites were identified (Figure 1B,D, bottom panel). Interestingly, two motifs (aa 99−119 and aa 158−181) are located in the major DNA binding domain (aa 87−187) of DEK and display a high degree of sequence homology to the established PAR-binding consensus motif (Figure 1B, PAR consensus). Another candidate binding site is located C-terminally adjacent to the major DNA-binding domain (aa 195−222). Two motifs (aa 314−334 and aa 329−352) were found in the C-terminal part of DEK, overlapping with the second DNA-binding or multimerization domain. Prompted by the sequence alignment, we synthesized corresponding DEK peptides to test for functional PAR binding using overlay slot blots (Figure 1C). Strikingly, DEK peptide 195−222 showed a strong PAR signal in a concentration-dependent manner starting at 50 pmol of PAR. A slightly weaker signal was detected using peptide 158−181, and rather weak binding was observed for C-terminal peptide 329−352. Peptides 99−119 and 314−334 failed to bind, even at high PAR concentrations. To further verify our peptide-derived results, we subjected selected recombinant DEK fragments, produced in bacteria (aa 68−226) or insect cells (aa 250−375 and aa 1−375), to the same approach (Figure 1D). DEK fragment 68−226, which comprises the two PAR-binding sites revealed by the peptide approach, produced a very strong signal (Figure 1D, 68−226, right panel). The second DEK fragment, 250−375 (Figure 1D, 250−375, right panel), showed a lower affinity for PAR comparable to that of wt-DEK (Figure 1D, 1−375). Wild-type DEK (wt-DEK) and fragment 250−375 were purified from insect cells and were therefore phosphorylated (see also Materials and Methods). We further compared PAR binding affinities of phosphorylated and dephosphorylated DEK and found an only slightly reduced overall PAR binding capacity for phosphorylated DEK (see Figure 4 A and Figure S2 of the Supporting Information). Another prominent band at ~35 kDa was observed in the wt-DEK preparation, which corresponds to a previously described N-terminal degradation product (*65*), and was visible in the protein staining of the individual protein preparations (Figure 1D, arrow). Additionally, an intermediate degradation product of unknown nature, present in the wt-DEK preparation, also bound efficiently to PAR (Figure 1D, asterisk). BSA failed to react with PAR (Figure 1D, BSA), underscoring the selectivity of this assay. Altogether, we have identified three functional PAR-binding sites in DEK by means of a peptide approach and confirmed the interaction using recombinant DEK fragments spanning the sites of interest.

DEK Exhibits a High Binding Affinity for Long PAR Chains. Having identified the regions for noncovalent PAR binding in the DEK molecule, we next investigated whether DEK exhibits any selectivity with respect to PAR chain length. Therefore, PAR was fractionated according to chain length by high-resolution HPLC as described recently (*18*), and the individual fractions were subsequently used in PAR overlay studies with purified recombinant DEK (Figure 2). For the sake of simplicity, five adjacent HPLC fractions were pooled, resulting in samples comprising approximately five distinct PAR chain lengths, i.e., 5−10, 11−15, etc. This was further verified by modified sequencing gel electrophoresis followed by silver staining (data not shown) of the pooled fractions. First, histone H1, known to exhibit chain-dependent PAR binding, was analyzed using the fractionated PAR preparations and clearly demonstrated chain length-dependent noncovalent interaction (Figure 2A). Oligo(ADP-ribose) molecules ranging from 5 to 10 units displayed weak affinity for histone H1, whereas longer polymers (starting with 15−19 units) or unfractionated PAR (1−*y*) was tightly

bound to the immobilized protein. The identical PAR preparations were then used to study binding to recombinant full-length DEK (Figure 2B). Binding of short PAR chains containing up to 39 units was very weak, with longer PAR chains, ranging from 34 to 54 units, showing slightly enhanced binding to DEK. In contrast, PAR containing more than 57 ADP-ribose units, or unfractionated PAR (1−*y*), showed an extremely high affinity for DEK, producing the strongest PAR signals. Results obtained with DEK and histone H1 were further analyzed by densitometry, and signal intensities confirm a clear preference of DEK for long PAR chains that exceeds that of histone H1 (Figure 2C).

To further validate this result, a PAR-specific EMSA approach using biotin-labeled polymers of defined sizes was used. First, specific end labeling of PAR was achieved by using a carbonyl-reactive biotin analogue, termed biocytin hydrazide, and was monitored by a neutravidin ELISA, which allows for the immobilization of biotinylated PAR chains. As a reference, a biotinylated standard (B-PAR) was synthesized in the presence of NAD^+ and 6-biotin-17-NAD^+, leading to the incorporation of biotinylated ADP-ribose units into the growing polymer chain. As little as 2.9 pmol of this standard was readily detectable (Figure 3A, left panel). Three different dilutions (171, 86, and 17 pmol) of end-biotinylated PAR samples were also applied and revealed biotin-coupled PAR in a concentration-dependent manner, whereas a 10-fold excess of unlabeled PAR displayed virtually no signal (data not shown). Additionally, efficient biotin labeling of these PAR polymers was confirmed by native PAGE and detection using streptavidin-POD (Figure 3A, right panel). End-labeled PAR was then separated by anion exchange HPLC according to chain length as described in Materials and Methods. Two PAR fractions (18mer and 54mer PAR) were selected and affinity-purified using a monomeric avidin column, and purification was monitored as described in Figure S1 of the Supporting Information. The concentration of the collected affinity-purified 18mer and 54mer PAR samples was determined in comparison with that a commercially available biotinylated 49mer oligonucleotide (Figure S1).

The two biotin-labeled size-fractionated PAR samples were then used to assess the binding to recombinant DEK (Figure 3B). Short 18mer PAR (250 fmol) was incubated in triplicate in the presence or absence of increasing amounts of recombinant DEK (0−1 μM) under EMSA conditions. DEK failed to mediate the formation of a specific complex with the 18mer PAR. A faint, slowly migrating complex is visible, starting with 0.1 μM DEK, and is due to minor cross contaminations with longer PAR chains that were introduced during the affinity purification procedure (Figure 3B, asterisk). Furthermore, high DEK concentrations led to a reduction of the signal intensity of free 18mer PAR, most likely caused by low-affinity binding to DEK. This was confirmed by prolonged exposure of the blot, which revealed a nonspecific smear at higher DEK concentrations (data not shown). In contrast, DEK at a concentration of 70 nM bound ~50% of the 54mer PAR and produced a defined, clearly identifiable, complex at concentrations starting with 100 nM DEK (Figure 3C). A DEK concentration of 200 nM also promoted the formation of a defined complex, which displayed a slightly reduced electrophoretic mobility as compared to incubation with 100 nM DEK. The signals were further quantitated densitometrically and revealed a strict dependency of PAR complex formation on DEK concentration (Figure 3D). The EMSA data obtained were subsequently used to calculate the K_D value for the interaction of DEK with long PAR chains (see also Figure S5 of the Supporting Information). The K_D value was in the low nanomolar range, indicative of high binding affinity (Table 1). It is noteworthy that DEK exhibits a higher affinity for long ADP-ribose chains compared to p53 and XPA. Similar to XPA, DEK was not capable of producing a defined complex with short ADP-ribose molecules (*18*).

Noncovalent PAR Modification Competitively Interferes with DNA in the Formation of DEK Multimers. We have recently reported that covalent poly(ADP-ribosyl)ation of DEK catalyzed by recombinant PARP-1 results in impaired general DNA binding, and, as a consequence, in the loss of DEK's supercoiling activity (*24*). In addition, we observed that the presence of PAR covalently bound to DEK disrupts DEK's ability to bind DNA via the SAP box-triggered "mass binding" mechanism, as measured by impaired formation of large nucleoprotein complexes in aggregation assays (*42*). As noted above, the recombinant His-DEK used in these experiments (Figures 1−3) was expressed in insect cells and purified in its phosphorylated form. As phosphorylation abolishes DEK's DNA binding activity (*36*, *37*), we had to dephosphorylate His-DEK before studying the impact of PAR on DEK's DNA binding activity (see also Materials and Methods) (*24*, *36*). Consequently, we first tested if the phosphorylation status of DEK influences its ability to bind to unfractionated, short chain or long chain PAR polymers. Using PAR overlay blots as described above, we observed a moderately reduced overall PAR binding capacity in phosphorylated DEK samples. However, phosphorylation did not influence the preferential binding selectivity for long chain PAR polymers. This binding selectivity for long PAR chains was equally visible in both DEK species (Figure 4A, α-PAR, and Figure S2 of the Supporting Information), thus validating the use of dephosphorylated DEK for further experiments.

First, we wanted to asses if PAR of various chain lengths alters the DNA binding properties of DEK. To discriminate between the direct interaction of DEK with DNA and its subsequent DNA-dependent multimerization activities, we initially employed immobilized DEK in a South-Western approach. Interestingly, dephosphorylated DEK (+PPase) bound to P^{32}-labeled DNA, regardless of prior incubation with unfractionated PAR, or PAR chains comprising 18 (PAR_{18}) or 53 (PAR_{53}) units (Figure 4A, left panel), even at concentrations of up to 600 nM (Figure S3 of the Supporting Information). As expected, phosphorylated DEK did not bind to DNA (*24*, *36*, *37*) but remained capable of interacting with PAR (Figure 4A, right panel).

Next, we assessed the influence of PAR on DEK's DNA binding in solution by standard EMSA techniques as previously described (*36*, *37*), now taking DEK's multimerization activity into consideration. Dephosphorylated His-DEK was incubated in the absence (Figure 4B, lane 1, and lanes 3−6) or presence of increasing concentrations of PAR [0, 100, 200, 400 (data not shown), or 600 nM (Figure 4B, lanes 7−10)] and subjected to native agarose gel electrophoresis (Figure 4B). As expected, DEK readily bound to DNA, with a preference for supercoiled DNA at lower DEK concentrations (*39*) [compare the ratios of form I (supercoiled) and form II (relaxed) in lane 4] and formed very large nucleoprotein complexes at higher DEK concentrations (e.g., lane 6, arrow). The latter effect is due to its DNA-dependent multimerization activity and ability to promote the formation of inter- and intramolecular interactions between DNA strands (*38*, *39*, *42*, *43*). Pretreatment of DEK with unfractionated PAR (600 nM) did not influence the overall DNA binding activity but appeared to slightly weaken the preference for supercoiled DNA forms (compare lane 4 to lane 8, white arrows). PAR itself had no

influence on the electrophoretic mobility of the utilized DNA (Figure 4B, lane 2).

We next wished to assess the impact of PAR binding on the ability of DEK to introduce positive supercoils into DNA templates. Therefore, we employed topology assays using negatively supercoiled Simian Virus 40 (SV40) DNA as a template (*38*).To visualize DEK-induced topological changes to DNA, topoisomerase I (Topo I) is present in this assay. Control experiments excluded the influence of PAR on topoisomerase I function (data not shown and Figure 5B, +Topo I, +PAR), as Topo I harbors three noncovalent PAR binding sites (*66*). As shown in Figure 5A, SV40 DNA is fully converted from its supercoiled form (form I) into the relaxed form (form II) in the presence of topoisomerase I (lane 2). Addition of increasing amounts of DEK resulted in well-defined, constrained DNA topoisomers (Figure 5A, lanes 3−5), reaching saturation at 800 ng of DEK (lane 5), which is indicated by a reduced intensity of supercoils in the lower part of the gel (compare lane 4 to lane 5) (*38*). Preincubation of DEK with different concentrations of unfractionated PAR [Figure 5A, 200 (lanes 6−8) or 600 nM PAR (lanes 9−11)] slightly affected this supercoilong activity, as no saturation was observed at the highest DEK concentration used (in Figure 5 A, compare lanes 5, 8, and 11, and see Figure S4 of the Supporting Information).

Full-length DEK induces positive supercoiling (*38*); however, Bohm et al. (*42*) have identified two domains in DEK (aa 68−87 and aa 187−208) that, upon deletion of either or both, result in a switch to negative DNA winding activity of DEK. Negative supercoils, as opposed to positive supercoils, favor local unwinding of the DNA double helix, thus facilitating processes such as transcription, DNA replication, and repair. Strikingly, the PAR binding motif with the strongest affinity identified [aa 195−222 (Figure 1)] overlaps with one of the switch domains. Noncovalent attachment of PAR could therefore modulate the function of this domain, possibly resulting in the negative supercoiling activity of DEK. To test for this hypothesis, we performed two-dimensional gel agarose electrophoresis (Figure 5B). As expected, incubation of SV40 DNA with DEK, followed by subsequent incubation with chloroquine in the second dimension, produced DNA topoisomers that migrate in a clockwise direction (positive supercoils, Figure 5B, +DEK, −PAR). This positive supercoiling activity of DEK was, however, not affected by the presence of PAR (Figure 5B, +DEK, +PAR). In summary, noncovalent interaction between PAR and DEK produces a subtle, negative effect on DEK's DNA binding activity. This negative effect becomes visible in solution assays (EMSA and topology assays). We considered that this may be evidence of a role for PAR in modulating DEK's self-interacting ability.

Therefore, we next employed an aggregation assay that allows us to measure this activity. We used this method, as described previously (*42*), to test if PAR modifies affinities of DEK for DNA molecules of variable superhelicity. Partially relaxed SV40 DNA [comprising SV40 DNA topoisomers ranging from 25 (form I, highly supercoiled) to 0 supercoils (form II, relaxed)] was incubated with increasing concentrations of dephosphorylated DEK, either in the presence or in the absence of 600 nM PAR, followed by centrifugation of the formed nucleoprotein complexes. The recovered pellet fractions (corresponding to bound DNA present in large nucleoprotein complexes) were then analyzed by gel electrophoresis. As shown before, full-length DEK binds efficiently to a wide range of superhelical DNA forms using this assay (Figure 6A,B, DEK). In the presence of PAR, the binding affinity of DEK for DNA topoisomers of high superhelicity was strongly reduced (Figure 6A,B, DEK+PAR). Furthermore, less DNA was precipitated overall. The decreased level of precipitation suggested weaker DNA binding, and interference of PAR with DEK's DNA-dependent multimerization activity. To further support this interpretation, we performed density gradients as reported previously (*36*, *37*). Recombinant His-DEK, either phosphorylated (Figure 6C, −PPase) or dephosphorylated (Figure 6C, +PPAse), was incubated in the presence or absence of 600 nM unfractionated PAR and subjected to sedimentation analysis. Surprisingly, PAR strongly augmented the formation of large DEK multimers beyond the phosphorylation-triggered multimerization activity (Figure 6B, top panels, −PPase, α-DEK) (*36*). This is underscored by the exclusive presence of PAR in the bottom fraction (Figure 6B, top panels, α-PAR). Importantly, the reduced abundance of DEK molecules in the top fractions coincided with a PAR-dependent accumulation. These large PAR-bound DEK complexes in the bottom fraction of the gradient were also observed with dephosphorylated DEK, however to a lesser extent (Figure 6B, lower panels, +PPase, α-DEK, α-PAR).

Taken together, the strong noncovalent interaction of PAR and DEK does not impair DEK's DNA binding per se; however, PAR seems to be able to replace DNA in catalyzing the formation of high-molecular mass DEK complexes.

DISCUSSION

In this study, we have dissected the noncovalent interaction of PAR, a complex biopolymer formed in response to genotoxic stress, and the oncoprotein DEK and studied its effect on DEK function. On the basis of our previous observation that DEK is capable of binding noncovalently to PAR, we set out to map the PAR-binding sites using a sequence alignment according to Pleschke et al. (*15*) in conjunction with PAR binding assays. This resulted in the identification of three functional PAR-binding sites within DEK's primary sequence, similar to the situation in tumor suppressor protein p53 (*19*). The binding affinity of DEK for PAR was slightly weaker compared to that of histone H1, which is among the strongest PAR binders, as judged by a slot-blot assay. Using size-fractionated PAR, we then showed that DEK preferably binds to longer PAR chains, which was also found for XPA (*18*), but differs from histone H1. The observed binding specificity was confirmed using a more sophisticated EMSA approach with size-fractionated, end-biotinylated PAR with a defined chain length. Long PAR molecules (54mer) produced a specific complex with DEK in a concentration-dependent manner, allowing for the determination of the K_D value (6×10^{-8} M), which is in the low nanomolar range. This binding affinity is even higher than those determined previously for p53 and XPA (*18*). Intriguingly, DEK was not capable of forming a defined complex with very short ADP-ribose molecules, which supports earlier observations that binding occurs as a function of chain length (*18*, *67*, *68*). The biological role of PAR chain length was previously underscored by Yu and colleagues, who demonstrated that PAR, depending on its chain length, can function as a death signal, leading to caspase-independent cell death (*69*, *70*).

It is well-known that noncovalent PAR binding may modulate the function of its target proteins. On one hand, PAR can positively regulate the enzymatic properties of its binding partner, e.g., an increased DNA joining activity of DNA ligase III (*20*) or activation of ATM kinase (*71*). On the other hand,

PAR also negatively affects the function of other interacting proteins, e.g., PAR-mediated inhibition of the DNA binding activity of p53 (*19*). This prompted us to study the effect of noncovalent PAR binding on DEK functions. Surprisingly, PAR concentrations of ≤600 nM did not influence the DNA binding of immobilized DEK, although an increase in negative charge might be expected to cause electrostatic repulsion and subsequent dissociation of DEK from DNA. Indeed, DEK can simultaneously bind PAR and DNA, as revealed by our South-Western blot experiments. This is in contrast to the covalent modification of DEK with PAR, which strongly inhibits its DNA binding activity (*24*). By further dissecting DEK's DNA binding activities, we found subtle, yet reproducible, effects of noncovalent PAR modifications on DEK's DNA binding activity in solution. PAR interfered weakly, yet measurably, with DEK's supercoiling activity. This occurred without causing a switch in the orientation of DNA winding. In contrast, we have previously shown that covalently modified DEK completely lost its ability to alter DNA topology (*24*). Importantly, we observed that PAR competitively suppressed DEK−DNA aggregation and, by promoting the self-interaction of DEK molecules, reduced the affinity of DEK for supercoiled DNA forms. Interestingly, this effect on DEK's multimerization was particularly pronounced using phosphorylated DEK but was also clearly evident in dephosphorylated DEK samples. Therefore, we speculate that noncovalent attachment of PAR to DEK may have two possible functions in the cell: (1) to further augment self-interaction of phosphorylated DEK molecules, which have already detached from DNA, and (2) to competitively counteract DNA binding, by favoring PAR-dependent formation of DEK multimers.

This may represent a mechanism of how noncovalently attached PAR impinges on DEK's spreading along chromatin fibers in a competitive manner. This modulation could play a role during DNA repair, as PAR-bound DEK might dissociate from supercoiled DNA at the site of a DNA lesion to allow repair and/or redistributes to adjacent sites of chromatin, where it may be stored in large complexes until the site of damage is cleared.

A growing body of evidence has linked the oncoprotein DEK to the DNA damage sensor PARP-1 and its product PAR, suggesting a functional interplay in PAR-dependent maintenance of genomic integrity and chromatin remodeling. Consistent with our findings described here and elsewhere (*24*), in silico analysis based on a refined consensus sequence as reported by Pleschke et al. (*15*) has also confirmed DEK as part of the PAR interaction network (*72*). Very recently, DEK was found in ecdysone-induced puffs, i.e., a local loosening of polytene chromatin in *Drosophila* (*73*). Interestingly, PARP-1 is required for the formation of normal-sized puffs, and elevated PAR levels were detected in ecdysone-dependent puffs (*74*). The chromatin relationship is further supported by the finding that both DEK and PARP-1 are present together in a chromatin fraction enriched for macrodomain-containing histone mH2A1.1 (*58*). Timinszky and colleagues recently reported that DEK, PARP-1, and mH2A1.1 are physically associated in HeLa cells and showed the PAR-mediated recruitment of mH2A1.1 to sites of laser-induced DNA damage, resulting in the modulation of chromatin structure (*75*). Therefore, it is tempting to speculate that PARP-1, DEK, and mH2A1.1 act in concert to spatially modulate chromatin structure and that this functional interplay is mediated by PAR, which binds to DEK and mH2A1.1. This could also explain the rather limited effect of PAR binding on DEK function in vitro described here, since PAR may be rather involved in the local recruitment of DEK to sites of DNA lesions, as shown for scaffold protein XRCC-1 (*21*, *76*), or may induce its redistribution to surrounding chromatin regions.

In summary, our findings reveal DEK as a potent PAR-binding protein that shows differential binding to PAR as a function of chain length. This strong noncovalent interaction does not affect DNA binding of DEK per se but may modulate functions that depend on the formation of larger DEK−DEK complexes. This is exemplified here by the competitive PAR-dependent modulation of DEK's selectivity for supercoiled DNA, which could be critical during DNA repair processes. This study contributes to the molecular understanding of the DEK−PAR interplay and further supports the existence of a cellular "PAR code".

ACKNOWLEDGMENT

We thank Prof. A. Marx and Dr. R. Kranaster (University of Konstanz) for kindly providing the HPLC facility and for support with the large-scale HPLC fractionation of PAR, Prof. M. Przybylski (University of Konstanz) for his advice and support with the peptide synthesis, and Prof. M. Miwa and Prof. T. Sugimura (Tokyo, Japan) for kindly providing 10H hybridoma cells.

SUPPORTING INFORMATION AVAILABLE

Avidin chromatography of end-biotinylated 18mer or 54mer PAR (Figure S1), PAR overlay blot using 100 nM PAR (Figure S2), South-Western analysis (Figure S3), magnified depiction of Figure 5A (Figure S4), and a graph depicting the determination of the K_D value (Figure S5). This material is available free of charge via the Internet at http://pubs.acs.org.

REFERENCES

1. Burkle, A. (2005) Poly(ADP-ribose). The most elaborate metabolite of NAD^+. *FEBS J. 272*, 4576–4589.
2. Ame, J. C., Spenlehauer, C., and de Murcia, G. (2004) The PARP superfamily. *BioEssays 26*, 882–893.
3. Shieh, W. M., Ame, J. C., Wilson, M. V., Wang, Z. Q., Koh, D. W., Jacobson, M. K., and Jacobson, E. L. (1998) Poly(ADP-ribose) polymerase null mouse cells synthesize ADP-ribose polymers. *J. Biol. Chem. 273*, 30069–30072.
4. D'Amours, D., Desnoyers, S., D'Silva, I., and Poirier, G. G. (1999) Poly(ADP-ribosyl)ation reactions in the regulation of nuclear functions. *Biochem. J. 342* (Part 2), 249–268.
5. Simbulan-Rosenthal, C. M., Haddad, B. R., Rosenthal, D. S., Weaver, Z., Coleman, A., Luo, R., Young, H. M., Wang, Z. Q., Ried, T., and Smulson, M. E. (1999) Chromosomal aberrations in PARP-(−/−) mice: Genome stabilization in immortalized cells by reintroduction of poly(ADP-ribose) polymerase cDNA. *Proc. Natl. Acad. Sci. U.S.A. 96*, 13191–13196.
6. Schreiber, V., Dantzer, F., Ame, J. C., and de Murcia, G. (2006) Poly(ADP-ribose): Novel functions for an old molecule. *Nat. Rev. Mol. Cell Biol. 7*, 517–528.
7. Kupper, J. H., Muller, M., and Burkle, A. (1996) Trans-dominant inhibition of poly(ADP-ribosyl)ation potentiates carcinogen induced gene amplification in SV40-transformed Chinese hamster cells. *Cancer Res. 56*, 2715–2717.
8. Meyer, R., Muller, M., Beneke, S., Kupper, J. H., and Burkle, A. (2000) Negative regulation of alkylation-induced sister-chromatid exchange by poly(ADP-ribose) polymerase-1 activity. *Int. J. Cancer 88*, 351–355.
9. Berger, F., Lau, C., and Ziegler, M. (2007) Regulation of poly(ADP-ribose) polymerase 1 activity by the phosphorylation state of the nuclear NAD biosynthetic enzyme NMN adenylyl transferase 1. *Proc. Natl. Acad. Sci. U.S.A. 104*, 3765–3770.
10. Bryant, H. E., Schultz, N., Thomas, H. D., Parker, K. M., Flower, D., Lopez, E., Kyle, S., Meuth, M., Curtin, N. J., and Helleday, T. (2005) Specific killing of BRCA2-deficient tumours with inhibitors of poly(ADP-ribose) polymerase. *Nature 434*, 913–917.

11. Flohr, C., Burkle, A., Radicella, J. P., and Epe, B. (2003) Poly(ADP-ribosyl)ation accelerates DNA repair in a pathway dependent on Cockayne syndrome B protein. *Nucleic Acids Res. 31*, 5332–5337.
12. Mitchell, J., Smith, G. C., and Curtin, N. J. (2009) Poly(ADP-Ribose) polymerase-1 and DNA-dependent protein kinase have equivalent roles in double strand break repair following ionizing radiation. *Int. J. Radiat. Oncol. Biol. Phys. 75*, 1520–1527.
13. Ame, J. C., Fouquerel, E., Gauthier, L. R., Biard, D., Boussin, F. D., Dantzer, F., de Murcia, G., and Schreiber, V. (2009) Radiation-induced mitotic catastrophe in PARG-deficient cells. *J. Cell Sci. 122*, 1990–2002.
14. Niere, M., Kernstock, S., Koch-Nolte, F., and Ziegler, M. (2008) Functional localization of two poly(ADP-ribose)-degrading enzymes to the mitochondrial matrix. *Mol. Cell. Biol. 28*, 814–824.
15. Pleschke, J. M., Kleczkowska, H. E., Strohm, M., and Althaus, F. R. (2000) Poly(ADP-ribose) binds to specific domains in DNA damage checkpoint proteins. *J. Biol. Chem. 275*, 40974–40980.
16. Ahel, I., Ahel, D., Matsusaka, T., Clark, A. J., Pines, J., Boulton, S. J., and West, S. C. (2008) Poly(ADP-ribose)-binding zinc finger motifs in DNA repair/checkpoint proteins. *Nature 451*, 81–85.
17. Gatz, S. A., and Wiesmuller, L. (2006) p53 in recombination and repair. *Cell Death Differ. 13*, 1003–1016.
18. Fahrer, J., Kranaster, R., Altmeyer, M., Marx, A., and Burkle, A. (2007) Quantitative analysis of the binding affinity of poly-(ADP-ribose) to specific binding proteins as a function of chain length. *Nucleic Acids Res. 35*, e143.
19. Malanga, M., Pleschke, J. M., Kleczkowska, H. E., and Althaus, F. R. (1998) Poly(ADP-ribose) binds to specific domains of p53 and alters its DNA binding functions. *J. Biol. Chem. 273*, 11839–11843.
20. Leppard, J. B., Dong, Z., Mackey, Z. B., and Tomkinson, A. E. (2003) Physical and functional interaction between DNA ligase IIIα and poly(ADP-Ribose) polymerase 1 in DNA single-strand break repair. *Mol. Cell. Biol. 23*, 5919–5927.
21. Okano, S., Lan, L., Caldecott, K. W., Mori, T., and Yasui, A. (2003) Spatial and temporal cellular responses to single-strand breaks in human cells. *Mol. Cell. Biol. 23*, 3974–3981.
22. Haince, J. F., Kozlov, S., Dawson, V. L., Dawson, T. M., Hendzel, M. J., Lavin, M. F., and Poirier, G. G. (2007) Ataxia telangiectasia mutated (ATM) signaling network is modulated by a novel poly-(ADP-ribose)-dependent pathway in the early response to DNA-damaging agents. *J. Biol. Chem. 282*, 16441–16453.
23. Kappes, F., Burger, K., Baack, M., Fackelmayer, F. O., and Gruss, C. (2001) Subcellular localization of the human proto-oncogene protein DEK. *J. Biol. Chem. 276*, 26317–26323.
24. Kappes, F., Fahrer, J., Khodadoust, M. S., Tabbert, A., Strasser, C., Mor-Vaknin, N., Moreno-Villanueva, M., Burkle, A., Markovitz, D. M., and Ferrando-May, E. (2008) DEK is a poly(ADP-ribose) acceptor in apoptosis and mediates resistance to genotoxic stress. *Mol. Cell. Biol. 28*, 3245–3257.
25. von Lindern, M., Poustka, A., Lerach, H., and Grosveld, G. (1990) The (6;9) chromosome translocation, associated with a specific subtype of acute nonlymphocytic leukemia, leads to aberrant transcription of a target gene on 9q34. *Mol. Cell. Biol. 10*, 4016–4026.
26. Carro, M. S., Spiga, F. M., Quarto, M., Di Ninni, V., Volorio, S., Alcalay, M., and Muller, H. (2006) DEK expression is controlled by E2F and deregulated in diverse tumor types. *Cell Cycle 5*, 1202–1207.
27. Grasemann, C., Gratias, S., Stephan, H., Schuler, A., Schramm, A., Klein-Hitpass, L., Rieder, H., Schneider, S., Kappes, F., Eggert, A., and Lohmann, D. R. (2005) Gains and overexpression identify DEK and E2F3 as targets of chromosome 6p gains in retinoblastoma. *Oncogene 24*, 6441–6449.
28. Khodadoust, M. S., Verhaegen, M., Kappes, F., Riveiro-Falkenbach, E., Cigudosa, J. C., Kim, D. S., Chinnaiyan, A. M., Markovitz, D. M., and Soengas, M. S. (2009) Melanoma proliferation and chemoresistance controlled by the DEK oncogene. *Cancer Res. 69*, 6405–6413.
29. Orlic, M., Spencer, C. E., Wang, L., and Gallie, B. L. (2006) Expression analysis of 6p22 genomic gain in retinoblastoma. *Genes, Chromosomes Cancer 45*, 72–82.
30. Wise-Draper, T. M., Allen, H. V., Thobe, M. N., Jones, E. E., Habash, K. B., Munger, K., and Wells, S. I. (2005) The human DEK proto-oncogene is a senescence inhibitor and an upregulated target of high-risk human papillomavirus E7. *J. Virol. 79*, 14309–14317.
31. Wise-Draper, T. M., Allen, H. V., Jones, E. E., Habash, K. B., Matsuo, H., and Wells, S. I. (2006) Apoptosis inhibition by the human DEK oncoprotein involves interference with p53 functions. *Mol. Cell. Biol. 26*, 7506–7519.
32. Wise-Draper, T. M., Mintz-Cole, R. A., Morris, T. A., Simpson, D. S., Wikenheiser-Brokamp, K. A., Currier, M. A., Cripe, T. P., Grosveld, G. C., and Wells, S. I. (2009) Overexpression of the cellular DEK protein promotes epithelial transformation in vitro and in vivo. *Cancer Res. 69*, 1792–1799.
33. Wise-Draper, T. M., Morreale, R. J., Morris, T. A., Mintz-Cole, R. A., Hoskins, E. E., Balsitis, S. J., Husseinzadeh, N., Witte, D. P., Wikenheiser-Brokamp, K. A., Lambert, P. F., and Wells, S. I. (2009) DEK proto-oncogene expression interferes with the normal epithelial differentiation program. *Am. J. Pathol. 174*, 71–81.
34. Mor-Vaknin, N., Punturieri, A., Sitwala, K., Faulkner, N., Legendre, M., Khodadoust, M. S., Kappes, F., Ruth, J. H., Koch, A., Glass, D., Petruzzelli, L., Adams, B. S., and Markovitz, D. M. (2006) The DEK nuclear autoantigen is a secreted chemotactic factor. *Mol. Cell. Biol. 26*, 9484–9496.
35. Ko, S. I., Lee, I. S., Kim, J. Y., Kim, S. M., Kim, D. W., Lee, K. S., Woo, K. M., Baek, J. H., Choo, J. K., and Seo, S. B. (2006) Regulation of histone acetyltransferase activity of p300 and PCAF by proto-oncogene protein DEK. *FEBS Lett. 580*, 3217–3222.
36. Kappes, F., Scholten, I., Richter, N., Gruss, C., and Waldmann, T. (2004) Functional domains of the ubiquitous chromatin protein DEK. *Mol. Cell. Biol. 24*, 6000–6010.
37. Kappes, F., Damoc, C., Knippers, R., Przybylski, M., Pinna, L. A., and Gruss, C. (2004) Phosphorylation by protein kinase CK2 changes the DNA binding properties of the human chromatin protein DEK. *Mol. Cell. Biol. 24*, 6011–6020.
38. Waldmann, T., Eckerich, C., Baack, M., and Gruss, C. (2002) The ubiquitous chromatin protein DEK alters the structure of DNA by introducing positive supercoils. *J. Biol. Chem. 277*, 24988–24994.
39. Waldmann, T., Baack, M., Richter, N., and Gruss, C. (2003) Structure-specific binding of the proto-oncogene protein DEK to DNA. *Nucleic Acids Res. 31*, 7003–7010.
40. Waldmann, T., Scholten, I., Kappes, F., Hu, H. G., and Knippers, R. (2004) The DEK protein: An abundant and ubiquitous constituent of mammalian chromatin. *Gene 343*, 1–9.
41. Devany, M., Kappes, F., Chen, K. M., Markovitz, D. M., and Matsuo, H. (2008) Solution NMR structure of the N-terminal domain of the human DEK protein. *Protein Sci. 17*, 205–215.
42. Bohm, F., Kappes, F., Scholten, I., Richter, N., Matsuo, H., Knippers, R., and Waldmann, T. (2005) The SAF-box domain of chromatin protein DEK. *Nucleic Acids Res. 33*, 1101–1110.
43. Alexiadis, V., Waldmann, T., Andersen, J., Mann, M., Knippers, R., and Gruss, C. (2000) The protein encoded by the proto-oncogene DEK changes the topology of chromatin and reduces the efficiency of DNA replication in a chromatin-specific manner. *Genes Dev. 14*, 1308–1312.
44. Aravind, L., and Koonin, E. V. (2000) SAP: A putative DNA-binding motif involved in chromosomal organization. *Trends Biochem. Sci. 25*, 112–114.
45. Gradwohl, G., Mazen, A., and de Murcia, G. (1987) Poly-(ADP-ribose) polymerase forms loops with DNA. *Biochem. Biophys. Res. Commun. 148*, 913–919.
46. Sastry, S. S., and Kun, E. (1990) The interaction of adenosine diphosphoribosyl transferase (ADPRT) with a cruciform DNA. *Biochem. Biophys. Res. Commun. 167*, 842–847.
47. Devany, M., Kotharu, N. P., and Matsuo, H. (2004) Solution NMR structure of the C-terminal domain of the human protein DEK. *Protein Sci. 13*, 2252–2259.
48. Soares, L. M., Zanier, K., Mackereth, C., Sattler, M., and Valcarcel, J. (2006) Intron removal requires proofreading of U2AF/3′ splice site recognition by DEK. *Science 312*, 1961–1965.
49. Cavellan, E., Asp, P., Percipalle, P., and Farrants, A. K. (2006) The WSTF-SNF2h chromatin remodeling complex interacts with several nuclear proteins in transcription. *J. Biol. Chem. 281*, 16264–16271.
50. Campillos, M., Garcia, M. A., Valdivieso, F., and Vazquez, J. (2003) Transcriptional activation by AP-2α is modulated by the oncogene DEK. *Nucleic Acids Res. 31*, 1571–1575.
51. Hollenbach, A. D., McPherson, C. J., Mientjes, E. J., Iyengar, R., and Grosveld, G. (2002) Daxx and histone deacetylase II associate with chromatin through an interaction with core histones and the chromatin-associated protein Dek. *J. Cell Sci. 115*, 3319–3330.
52. Gamble, M. J., and Fisher, R. P. (2007) SET and PARP1 remove DEK from chromatin to permit access by the transcription machinery. *Nat. Struct. Mol. Biol. 14*, 548–555.
53. Fu, G. K., Grosveld, G., and Markovitz, D. M. (1997) DEK, an autoantigen involved in a chromosomal translocation in acute myelogenous leukemia, binds to the HIV-2 enhancer. *Proc. Natl. Acad. Sci. U.S.A. 94*, 1811–1815.
54. Faulkner, N. E., Hilfinger, J. M., and Markovitz, D. M. (2001) Protein phosphatase 2A activates the HIV-2 promoter through enhancer elements that include the pets site. *J. Biol. Chem. 276*, 25804–25812.

55. Tabbert, A., Kappes, F., Knippers, R., Kellermann, J., Lottspeich, F., and Ferrando-May, E. (2006) Hypophosphorylation of the architectural chromatin protein DEK in death-receptor-induced apoptosis revealed by the isotope coded protein label proteomic platform. *Proteomics 6*, 5758–5772.
56. Cleary, J., Sitwala, K. V., Khodadoust, M. S., Kwok, R. P., Mor-Vaknin, N., Cebrat, M., Cole, P. A., and Markovitz, D. M. (2005) p300/CBP-associated factor drives DEK into interchromatin granule clusters. *J. Biol. Chem. 280*, 31760–31767.
57. Tanuma, S., Kawashima, K., and Endo, H. (1985) Comparison of ADP-ribosylation of chromosomal proteins between intact and broken cells. *Biochem. Biophys. Res. Commun. 127*, 896–902.
58. Ouararhni, K., Hadj-Slimane, R., Ait-Si-Ali, S., Robin, P., Mietton, F., Harel-Bellan, A., Dimitrov, S., and Hamiche, A. (2006) The histone variant mH2A1.1 interferes with transcription by down-regulating PARP-1 enzymatic activity. *Genes Dev. 20*, 3324–3336.
59. Kawamitsu, H., Hoshino, H., Okada, H., Miwa, M., Momoi, H., and Sugimura, T. (1984) Monoclonal antibodies to poly(adenosine diphosphate ribose) recognize different structures. *Biochemistry 23*, 3771–3777.
60. Malanga, M., Bachmann, S., Panzeter, P. L., Zweifel, B., and Althaus, F. R. (1995) Poly(ADP-ribose) quantification at the femtomole level in mammalian cells. *Anal. Biochem. 228*, 245–251.
61. Shah, G. M., Poirier, D., Duchaine, C., Brochu, G., Desnoyers, S., Lagueux, J., Verreault, A., Hoflack, J. C., Kirkland, J. B., and Poirier, G. G. (1995) Methods for biochemical study of poly(ADP-ribose) metabolism in vitro and in vivo. *Anal. Biochem. 227*, 1–13.
62. Cheung, A., and Zhang, J. (2000) A scintillation proximity assay for poly(ADP-ribose) polymerase. *Anal. Biochem. 282*, 24–28.
63. Kiehlbauch, C. C., Aboul-Ela, N., Jacobson, E. L., Ringer, D. P., and Jacobson, M. K. (1993) High resolution fractionation and characterization of ADP-ribose polymers. *Anal. Biochem. 208*, 26–34.
64. Alvarez-Gonzalez, R., and Jacobson, M. K. (1987) Characterization of polymers of adenosine diphosphate ribose generated in vitro and in vivo. *Biochemistry 26*, 3218–3224.
65. Sierakowska, H., Williams, K. R., Szer, I. S., and Szer, W. (1993) The putative oncoprotein DEK, part of a chimera protein associated with acute myeloid leukaemia, is an autoantigen in juvenile rheumatoid arthritis. *Clin. Exp. Immunol. 94*, 435–439.
66. Malanga, M., and Althaus, F. R. (2004) Poly(ADP-ribose) reactivates stalled DNA topoisomerase I and Induces DNA strand break resealing. *J. Biol. Chem. 279*, 5244–5248.
67. Althaus, F. R., Bachmann, S., Hofferer, L., Kleczkowska, H. E., Malanga, M., Panzeter, P. L., Realini, C., and Zweifel, B. (1995) Interactions of poly(ADP-ribose) with nuclear proteins. *Biochimie 77*, 423–432.
68. Panzeter, P. L., Realini, C. A., and Althaus, F. R. (1992) Noncovalent interactions of poly(adenosine diphosphate ribose) with histones. *Biochemistry 31*, 1379–1385.
69. Yu, S. W., Wang, H., Poitras, M. F., Coombs, C., Bowers, W. J., Federoff, H. J., Poirier, G. G., Dawson, T. M., and Dawson, V. L. (2002) Mediation of poly(ADP-ribose) polymerase-1-dependent cell death by apoptosis-inducing factor. *Science 297*, 259–263.
70. Andrabi, S. A., Kim, N. S., Yu, S. W., Wang, H., Koh, D. W., Sasaki, M., Klaus, J. A., Otsuka, T., Zhang, Z., Koehler, R. C., Hurn, P. D., Poirier, G. G., Dawson, V. L., and Dawson, T. M. (2006) Poly(ADP-ribose) (PAR) polymer is a death signal. *Proc. Natl. Acad. Sci. U.S.A. 103*, 18308–18313.
71. Goodarzi, A. A., and Lees-Miller, S. P. (2004) Biochemical characterization of the ataxia-telangiectasia mutated (ATM) protein from human cells. *DNA Repair 3*, 753–767.
72. Gagne, J. P., Isabelle, M., Lo, K. S., Bourassa, S., Hendzel, M. J., Dawson, V. L., Dawson, T. M., and Poirier, G. G. (2008) Proteome-wide identification of poly(ADP-ribose) binding proteins and poly-(ADP-ribose)-associated protein complexes. *Nucleic Acids Res. 36*, 6959–6976.
73. Sawatsubashi, S., Murata, T., Lim, J., Fujiki, R., Ito, S., Suzuki, E., Tanabe, M., Zhao, Y., Kimura, S., Fujiyama, S., Ueda, T., Umetsu, D., Ito, T., Takeyama, K., and Kato, S. (2010) A histone chaperone, DEK, transcriptionally coactivates a nuclear receptor. *Genes Dev. 24*, 159–170.
74. Tulin, A., and Spradling, A. (2003) Chromatin loosening by poly-(ADP)-ribose polymerase (PARP) at *Drosophila* puff loci. *Science 299*, 560–562.
75. Timinszky, G., Till, S., Hassa, P. O., Hothorn, M., Kustatscher, G., Nijmeijer, B., Colombelli, J., Altmeyer, M., Stelzer, E. H., Scheffzek, K., Hottiger, M. O., and Ladurner, A. G. (2009) A macrodomain-containing histone rearranges chromatin upon sensing PARP1 activation. *Nat. Struct. Mol. Biol. 16*, 923–929.
76. El-Khamisy, S. F., Masutani, M., Suzuki, H., and Caldecott, K. W. (2003) A requirement for PARP-1 for the assembly or stability of XRCC1 nuclear foci at sites of oxidative DNA damage. *Nucleic Acids Res. 31*, 5526–5533.